IL NUOVO CIMENTO **40 C** (2017) 95
DOI 10.1393/ncc/i2017-17095-4

COMMUNICATIONS: SIF Congress 2016

Interseismic coupling for the Altotiberina Fault from GPS data

LETIZIA ANDERLINI(*)
INGV, Centro Nazionale Terremoti - Bologna, Italy

received 28 February 2017

Summary. — The Umbria-Marche Apennines is a region characterized by strong historical and instrumental earthquakes located in a complex tectonic framework where both extensional and compressional activities are taken up. Moreover a particular fault structure, the Altotiberina fault (ATF), seems to play an active role within this tectonic extension, even if it is still not clear whether this structure is active or able to generate big earthquakes. Nevertheless which of the known fault systems play a major role in accommodating the extension, and which are the modes (seismic VS aseismic deformation) this extension is taken up, are still debated topics. Using a dense network of high-precision GPS measurements and a kinematic block modeling approach, this study evaluates which fault systems can better explain the crustal deformation observed by geodetic data. Inferring a tectonic activity of the ATF within this context, we evaluate its interseismic coupling distribution, and the resolution capability due to the spatial distribution of data. A wide portion of ATF, well resolved by data, is aseismically creeping, whereas for the first 4–5 km of depth seems fully locked, providing new clues on its seismic potential.

1. – Introduction

Thanks to the fast improvement of high-resolution GPS measurements of ground deformation, it is possible to observe sub-mm deformation gradients that may provide accurate information about the fault seismogenic potential. Assuming faults embedded in an elastic brittle medium (good approximation for the first 10–15 km of the crustal thickness), the horizontal strain rate pattern observed by geodetic measurements is representative of how fault structures accommodate the tectonic deformation. This deformation may be released in two principal ways, *i.e.* by a seismic response occurring when the elastic strength of the crust surrenders, or by continuous aseismic low-friction creeping faults. Both cases generate a specific deformation pattern, whose kinematic study allows to estimate the involved fault geometry and how the deformation is accommodated.

(*) E-mail: letizia.anderlini@ingv.it

This study is focused to understand which fault systems are involved to explain the geodetic deformation field observed in Umbria-Marche Apennines (fig. 1), characterized mainly by SW-NE oriented extensional deformation, as documented by geodetic [1], geologic [2] and seismological [3] data. Most of the major historical and instrumental earthquakes [4] occurred mainly on the western side of the chain, bounded by west-dipping buried high-angle normal faults [5]. Moreover recent studies about the northernmost part of the Umbria-Marche region show seismic and tectonic activity [6, 7] in correspondence of the Altotiberina (AT) low-angle normal fault (LANF), which is widely documented by geological data [8] and deep seismic reflection profiles (*e.g.* CROP03) [9]. The ATF dimensions and position are well constrained by the interpretation of seismic reflection data [10], and it extends over a length of $\sim$ 70 km with an average inclination of 20° towards NE [6, 7, 11].

LANFs are very low dipping ($< 30°$) faults, that have been documented in various tectonic settings affected by crustal extension [12], whose geological evidence highlights a brittle-frictional behavior. Nevertheless, for the "Andersonian" theory, they should be considered averse to faulting, since they are misoriented with respect to the regional stress field [13]. In order to explain LANFs seismic activity, the most likely proposed hypothesis is considering the presence of fluid overpressures producing a fault frictional weakening [14]. This condition has been documented for the ATF from boreholes observations and it is generated by degassing of CO_2-saturated fluid, due to a deeply constant mantle flux [15]. The fluid triggering however may generate only short-time frictional instabilities, giving just a local stress variation enough for the nucleation of microseismicity [6]. Given the peculiarity of the case, a multidisciplinary near fault research infrastructure (TABOO, [16]) is operating as a part of the European Plate Observing System (`https://www.epos-ip.org`) Near Fault Observatories.

In this context GPS measurements may provide important information on the occurring active extension indicated by velocity gradients. During last years in the Umbria-Marche Apennines close to Gubbio fault (GuF, fig. 1) a dense network of continuous GPS stations, belonging to the RING-INGV network, has been installed, improving significantly the spatial resolution of the detectable geodetic deformations. Using the kinematic block modeling approach we evaluate which particular fault systems may justify the observed velocity field in this sector of the Apennines, and in particular we demonstrate the active kinematic role of the Alto Tiberina fault (ATF) within this tectonic context.

2. – GPS data

GPS measurements allows to obtain 3D position with high precision and continuity through time of a specific point. GPS velocities have been obtained from raw data recorded by several operating GPS networks in the Euro-Mediterranean and African regions, belonging to two acquisition strategies: survey-mode (EGPS) and continuous (CGPS) sites. These data have been analyzed by adopting a three-step approach, as described on [17], allowing to obtain a final position time series from which it is possible to estimate a long-term linear trend due to the occurring tectonic deformations. In particular the raw data analysis includes:

- estimate of site position, adjustments to satellite orbital parameters, timevariable piecewise linear zenith and horizontal gradient tropospheric delay parameters from daily GPS phase observations, using the GAMIT software [18] and applying loose constraints to geodetic parameters;

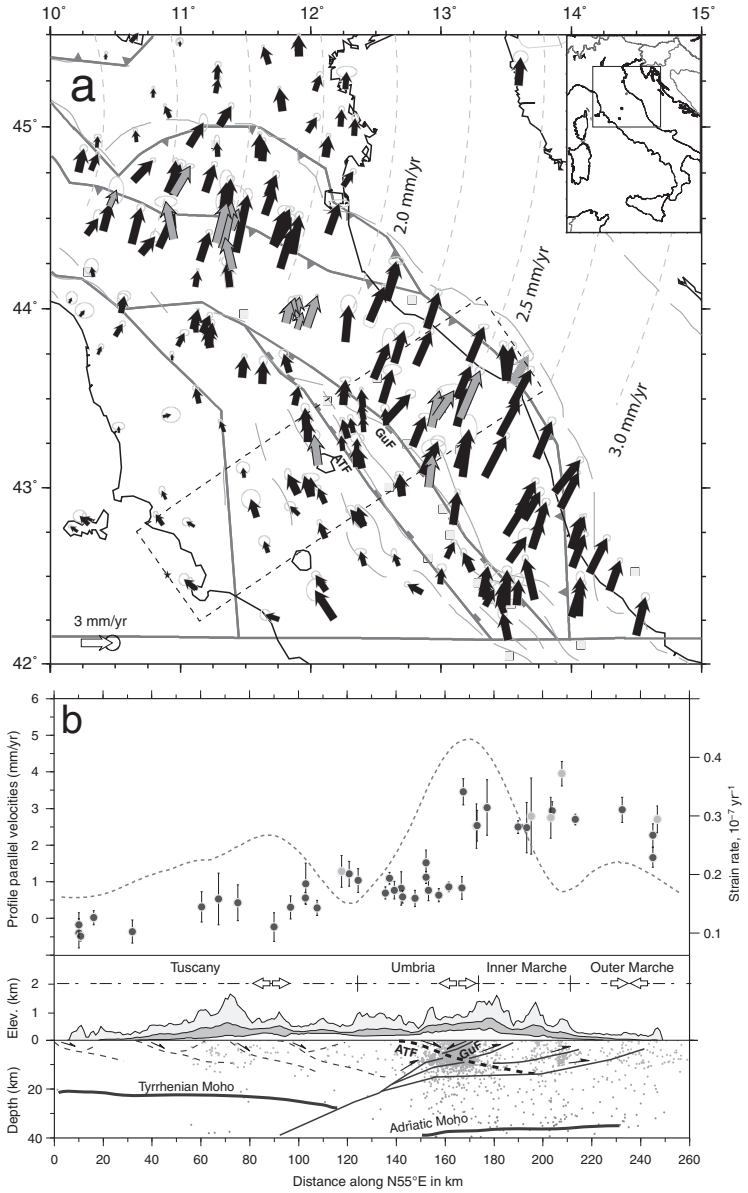

Fig. 1. – Seismotectonic framework for the Umbria-Marche Apennines. (a) Horizontal CGPS (black arrows) and EGPS (gray arrows) velocity field with respect to the Eurasian reference frame where the coherent rotation movement of the Adriatic domain (dashed curves) is reported; bold gray lines indicate the final block configuration following the main known fault systems ([5], light gray lines). (b) (Top) profile parallel components of GPS velocities with 1σ error bars along the cross section in panel a (dashed box), where the main gradients are highlighted by the strain-rate maxima (dashed line); (bottom) topography and cross section view of the subsurface structures and instrumental seismicity (gray dots), white arrows indicate the known tectonic regimes (compressional or extensional) of the different geographic provinces (after [19]).

- combination of all the daily loosely constrained solutions, for both cGPS and sGPS subnets, with the global solutions of the IGS network made available by SOPAC (`http://sopac.ucsd.edu`), realizing a global reference frame with respect to GPS position time series are provided;
- analysis of the position time series for the CGPS and EGPS stations, in order to estimate a constant linear velocity term together with annual and semi-annual seasonal components and, if present, offsets at specific epochs, adopting also white and flicker noise filtering and Common Mode Error (CME) removing.

The final GPS velocity field used in this study is partially shown in fig. 1(a), where the horizontal components are reported in a fixed-Eurasian reference frame, as a local reference frame that allows to identify most of the occurring tectonic deformation features. The velocity field shows clearly the coherent counterclockwise rotation of the Adriatic domain (dashed circle arcs in fig. 1(a)) moving slower with respect to the Appeninic chain, indicating the active compression along the easternmost buried thrusts systems. As highlighted in fig. 1(b) (profile parallel components of GPS velocities) we observe across this sector of the Northern Apennines a SW-NE extension of $\sim 3\,\mathrm{mm/yr}$ that is partially taken up in the Tuscany portion, and mostly across the Umbria-Marche boundary, as also illustrated by a strain-rate pattern (dashed line). In this study we used data from CGPS and EGPS stations with an observation period longer than 2.5 years, as shorter intervals may result in biased estimates of linear velocities [20].

3. – Block modeling approach

The Block Modeling theory (*e.g.* [21]) is a kinematic approach for which the velocity field observed by geodetic measurements is modeled considering the crust subdivided into plates, assumed as elastic rigid *blocks* rotating independently with respect to a reference one. Block boundaries are represented by rectangular fault planes embedded in an elastic, homogeneous and isotropic half-space [22] and their interactions caused by plate movements are associated to the observed velocity gradients. This simplified representation follows the *back-slip* concept explained by [23], which is based on the assumption that the sum of interseismic, $\mathbf{V_I}$, and coseismic, $\mathbf{V_E}$, deformations gives back the long-term motion of blocks, $\mathbf{V_B}$. So rearranging the terms, we can model the interseismic deformation as the sum of the long-term relative block motion (depending linearly on their angular velocity vectors, $\mathbf{\Omega}$) and a shallow long-term slip-rate acting on the opposite direction of coseismic slip sense (*i.e.* back-slip, see fig. 2). Also this last contribution depends linearly on the relative rotations of bounding blocks, so the block angular velocity vector ($\mathbf{\Omega}$, eq. (1)) contains the unknown parameters of the problem setting, and the estimated long-term slip rates, V_0 for the fault boundaries can be considered "self-consistent" within the whole kinematic framework:

$$\mathbf{V_I} = \mathbf{V_B} - \mathbf{V_E} = \mathbf{V} \cdot \Omega. \tag{1}$$

In a more complicated configuration, we can consider a spatial distribution of back-slip on a specific fault plane, better evaluating its seismic potential. This allows to identify in which part of the fault surface the elastic contribution should occur, *i.e.* distinguishing between the locked seismic "asperities" from the aseismic portions where interseismic "creep" occur at the same rate of the relative blocks rotation. In this case the fault is divided in subplanes (or patches) whose back-slip values, $\mathbf{s}$, are all independent

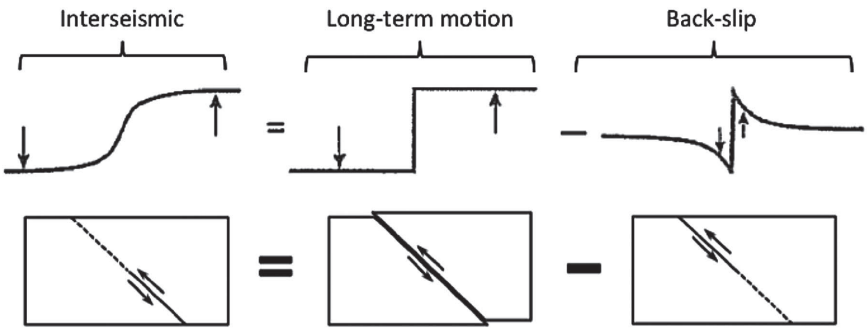

Fig. 2. – Back-slip approach within the block model representation. Top row: expected ground deformation patterns for each contribution; bottom row: schematic representation of relative blocks movements for the three terms.

unknowns, for which is applied a regularization operator allowing for slip continuity between neighboring elements. In this case eq. (1) becomes

$$\mathbf{V_I} = \mathbf{V_B} - \mathbf{V_E} - \mathbf{V_T} = \mathbf{V'} \cdot \begin{bmatrix} \mathbf{\Omega} \\ \mathbf{s} \end{bmatrix}, \tag{2}$$

where $\mathbf{V_T}$ is the elastic deformation due to discretized faults, whose back-slip values $\mathbf{s}$ are unknown parameters to estimate. In both eqs. (1) and (2), $\mathbf{V}$ and $\mathbf{V'}$ are linear operators containing geometrical conversions, dislocation Green's fuctions, smoothing contraints and weighting matrixes [24].

In this second case it is possible to estimate the *interseismic coupling* degree, Φ, calculated as the ratio between the slip deficit $\mathbf{s}$ (*i.e.* back-slip of each patch) during the interseismic period and the long-term slip rate V_0 derived from the relative motion of blocks. Φ varies between 0, where there is no slip deficit and the fault surface is aseismically creeping (uncoupled), and 1, where the back-slip value is close to the long-term relative block motion, indicating a fully coupled fault patch representing an asperity.

In order to retrieve the unknown parameters and to reproduce the geodetic velocity field, we use the block modeling implementation of [24], that use a weighted linear least squares (LLS) inversion method, and a regularization operator (*i.e.* second derivatives Laplacian) for the coupling distribution weighted by a factor β defined from a trade-off curve analysis [25]. The code has been modified in the case of the coupling distribution estimate, applying a linear constrained algorithm (LCA) based on the preconditioned conjugate gradient method [26], that allows to bound the back-slip values to be at the most equal to the long-term slip V_0.

4. – Block modeling analysis

The crustal deformation measured by GPS data (fig. 1(a)) has been reproduced using a wide block model geometry, in order to describe the overall motion of the Tyrrhenian and Adriatic domains, and to identify the role of the ATF and other faults in accommodating the measured crustal extension. We use seismotectonics, geodetic and geological/geophysical information, and maps of active faults (see [5] and reference therein) in order to develop the blocks configuration, defining dips and locking depths of the block-bounding faults represented as planar rectangular dislocations.

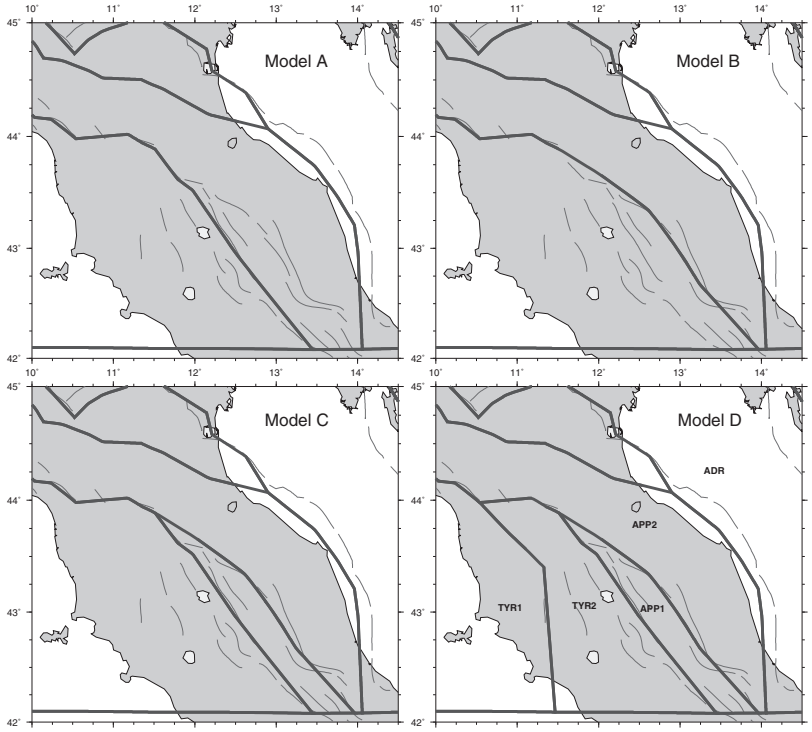

Fig. 3. – Four different configurations of block models tested to better reproduce the geodetic measurements of tectonic gradients.

Four different block model settings, more and more complicated, have been tested (fig. 3). Starting from models where only the ATF (Model A) or the Gubbio fault, GuF, (Model B) systems accommodate the long-term extension, we consider a model where both fault systems are active (Model C) and a further one accounting for extension in Tuscany (Model D). As the number of blocks grows, we evaluate their statistical acceptance by means of the F-ratio test [27] from decreasing χ^2 values of residuals. Results are reported in table I where the most complex model (D) provides not only the lowest residuals, but also a good statistical acceptance. This best block model configuration allows to infer that the tectonic extension should be accommodated by at least three

TABLE I. – *Statistical F-test results. For each model are reported: residual χ^2, number of blocks, F-ratio for more complicated models, the F-ratio minimum value for the statistical acceptance.*

Model name	χ^2	n. Blocks	F-ratio	F_{min} (99% conf.)
Model A	2317.29	10	–	–
Model B	2293.77	10	–	–
Model C	2217.25	11	A → C: 13.82 B → C: 10.57	3.81
Model D	1825.01	12	C → D: 65.62	3.81

different fault systems, providing also geodetic long-term slip rates for the ATF and GuF close to geological estimates.

5. – ATF interseismic coupling

Using the block model configuration D, we develop a more complicated setting allowing for the estimate of a back-slip spatial distribution for the Altotiberina fault. We discretize the fault surface into triangular dislocation elements (TDEs) refining its non-planar geometry by exploiting the high-resolution depth contour isobaths obtained by geological and geophysical data [7]. We used the LCA inversion approach, bounding the ATF back-slip values to be at the most equal to the long-term value found in the previous configuration. We constrain the slip-rate to taper to zero at the bottom of the ATF surface, at a depth of $\sim$ 13 km, roughly corresponding to the proposed brittle-ductile transition for this region [28]. We represent the results in terms of interseismic coupling degree ϕ (fig. 4(a)), obtaining a heterogeneous distribution along the fault surface. The main coupling features highlight that the shallow part is almost uniformly locked up to 4-5 km of depth (values close to 1) and the presence of a further locked asperity in a deeper portion of the fault. Overall, more that 50% of the fault surface is characterized by creeping behavior (values close to 0), finding a good correlation with the relocated microseismicity [6] which can be ascribed to aseismic stable-sliding behavior (*e.g.* [29]).

5˙1. *Resolution analysis.* – We evaluate how much of the inverted coupling distribution is resolved by data estimating the resolution length (RL, fig. 4(b)), which is the characteristic size of back-slip contribution that can be detected by the geodetic data [30] and it is computed for each TDE. To consider as resolved a coupling spatial feature, the RL should be constant on it and smaller than the feature size itself. In general, the surface elastic signal caused by a TDE located at shallow depths has a very short wavelength (few km) and can be potentially resolved only by very close GPS measurements. A longer wavelength characterizes the signal associated to a deeper TDE, which can be detectable also by sparser networks.

Figure 4(b) shows that at shallow depths the RL of the ATF can be as good as 2 km, mainly below the denser portion of the geodetic network, but far from the data it may attain values greater than 15 km, as we obtain for the southern and western shallow fault portions and the deeper one to the North.

In light of this analysis our data seems to provide a good resolution about the central shallow locked fault portion, whose lateral extensions are not well constrained, but can reasonably be expected due to the completely absence of microseismicity below 4 km of depth. Moreover the wide deep fault portion characterized by aseismic creep seems well justified by the data, and further corroborated by the microseismicity distribution. For what concern the northern deep fault portion the RL shows values comparable to the deeper asperity size, inferring that it may indicate the presence of a locked portion whose shape might be not completely constrained.

6. – Conclusions

Thanks to the fast improvement of the high-precision geodetic measurements, we have been able to provide new constraints on how and where the observed tectonic extension across the Umbria-Marche Apennines may be released. In particular using a block modeling approach we demonstrate that at least three fault systems from the Tyrrhenian sector

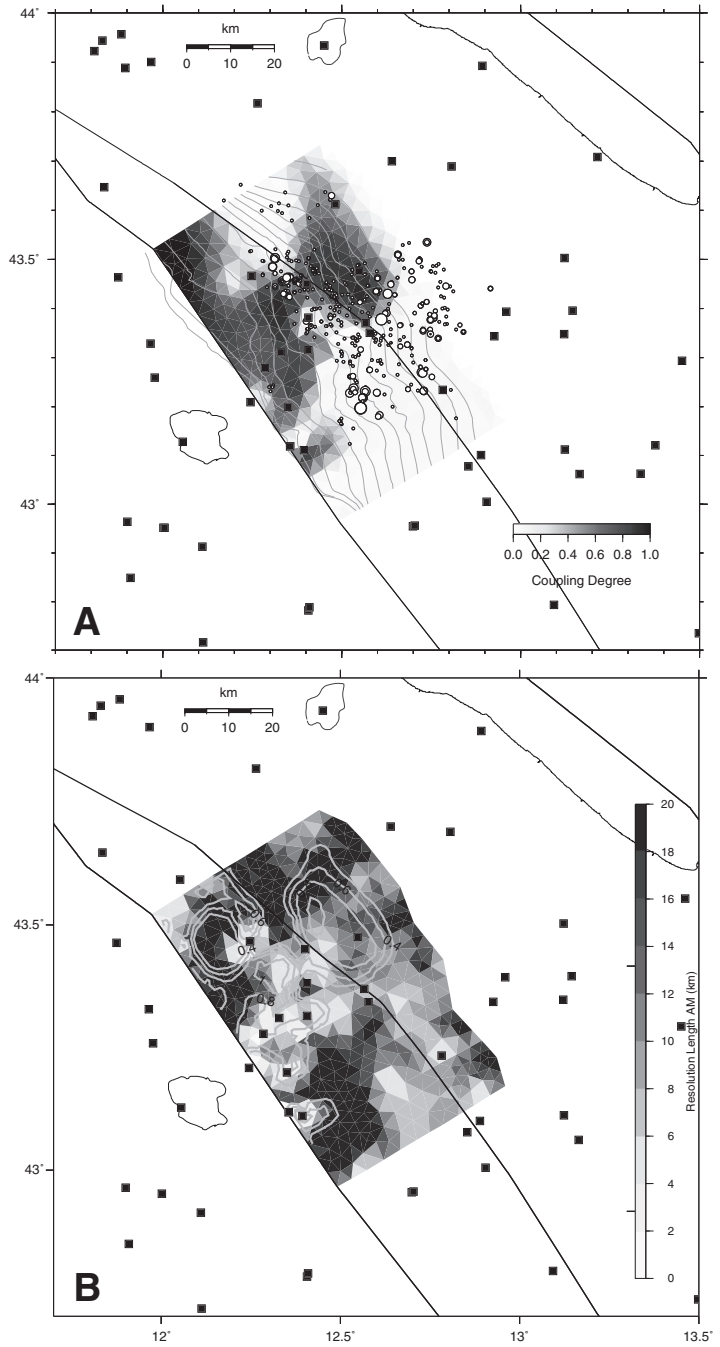

Fig. 4. – A: ATF interseismic coupling distribution with white circles representing the relocated microseismicity [6] and thin gray lines indicating the depth contour isobaths [7]. B: Resolution length with the interseismic coupling contour overlapped (light gray lines). For both panels black squares show GPS stations and the black segments are the fault-bounding blocks.

to the Adriatic one are actively accommodating the extensional deformation, obtaining two important results: 1) a subdivision of the Tyrrhenian-Tuscany domain whose active faults and their seismogenic potential remain debated; 2) a geodetically proven kinematic activity of the Altotiberina fault, although it belongs to a fault category (LANFs) that should be prevented to be seismically active.

The dense high-precision GPS measurements allow to provide the first image of spatially variable interseismic coupling on a LANF. The results indicate that the ATF is mainly locked down to a depth of 4–5 km, identifying also a deeper asperity located between 7 and 10 km of depth. On the other hand, the largest part of the fault surface turns out to be aseismically creeping, correlating with the relocated microseismicity. The resolution analysis provide a further check on the reliability of the ATF coupling distribution, providing new important clues for the seismic potential estimate to ascribe to this LANF, and consequently for the seismic hazard evaluation of the region.

* * *

This work has been developed in close collaboration with Maria Elina Belardinelli and Enrico Serpelloni, whom I thank for their indispensable support. I would also thank all the colleagues with whom I had constructive discussions about this controversial argument, *i.e.* Francesco Mirabella, Cristiano Collettini, Giovanni Chiodini, Romano Camassi, Luisa Valoroso and Luigi Vadacca. A special thanks is addressed to Lauro Chiaraluce for the several opinion exchanges and because he is strongly committed to develop the multidisciplinary Near Fault Observatory in the TABOO project. I would also thank Claudio Chiarabba, as a former director of the INGV Earthquake Sector, for providing me the necessary funds to attend the 2016 SIF conference.

REFERENCES

[1] D'Agostino N. *et al.*, *Tectonophysics*, **476** (2009) 3.
[2] Boncio P. and Lavecchia G., *J. Geodyn.*, **29** (2000) 233.
[3] Pondrelli S. *et al.*, *Phys. Earth Planet. Inter.*, **159** (2006) 286.
[4] Rovida A., Camassi R., Gasperini P. and Stucchi M. (Editors), *CPTI11, the 2011 version of the Parametric Catalogue of Italian Earthquakes* (Istituto Nazionale di Geofisica e Vulcanologia (INGV), Milano, Bologna) 2011, doi: 10.6092/INGV.IT-CPTI11.
[5] *Database of Individual Seismogenic Sources Working Group* (Istituto Nazionale di Geofisica e Vulcanologia (INGV)) 2015, `http://diss.rm.ingv.it/diss/`.
[6] Chiaraluce L. *et al.*, *J. Geophys. Res.*, **112** (2007) B10310.
[7] Mirabella F., Brozzetti F., Lupattelli A. and Barchi M. R., *Tectonics*, **30** (2011) TC6002.
[8] Brozzetti F., *Stud. Geol. Camerti*, **1** (1995) 105.
[9] Barchi M., Minelli G. and Pialli G., *Mem. Soc. Geol. Ital.*, **52** (1998) 383.
[10] Pialli G., Barchi M. and Minelli G., *Mem. Soc. Geol. Ital.*, **52** (1998) 1.
[11] Boncio P., Brozzetti F. and Lavecchia G., *Tectonics*, **19** (2000) 1038.
[12] Collettini C., *Tectonophysics*, **510** (2011) 253.
[13] Sibson R. H., *J. Struct. Geol.*, **7** (1985) 751.
[14] Collettini C., *Ann. Geophys.*, **45** (2002) 5.
[15] Chiodini G. *et al.*, *Geophys. Res. Lett.*, **31** (2004) L07615.
[16] Chiaraluce L. *et al.*, *Ann. Geophys.*, **57** (2014) S0327.
[17] Serpelloni E. *et al.*, *J. Geophys. Res. Solid Earth*, **118** (2013) 6003.
[18] Herring T., King R. W. and McClusky S., *GAMIT Reference Manual, Release 10.4* (Massachussetts Institute of Technology, Cambridge, MA) 2010.

[19] Anderlini L., Serpelloni E. and Belardinelli M. E., *Geophys. Res. Lett.*, **43** (2016) 4321.
[20] Blewitt G. and Lavallee D., *J. Geophys. Res.*, **107** (2002) 2145.
[21] McCaffrey R., *AGU Monograph*, **1** (2002) 1.
[22] Okada Y., *Bull. Seismol. Soc. Am.*, **75** (1985) 1135.
[23] Savage J. C., *J. Geophys. Res.*, **88** (1983) 4984.
[24] Meade B. J. and Loveless J. P., *Bull. Seismol. Soc. Am.*, **99** (2009) 3124.
[25] Harris R. A. and Segall P., *J. Geophys. Res.*, **92** (1987) 7945.
[26] Coleman T. F. and Verma A., *Comput. Optim. Appl.*, **20** (2001) 61.
[27] Stein S. and Gordon R., *Earth Planet. Sci. Lett.*, **69** (1984) 401.
[28] Boncio P., Lavecchia G. and Pace B., *J. Seismol.*, **8** (2004) 407.
[29] Sammis C. G. and Rice J. R., *Bull. Seismol. Soc. Am.*, **91** (2001) 532.
[30] Ader T. *et al.*, *J. Geophys. Res.*, **117** (2012) B04403.